Journal of Power Sources 195 (2010) 5882–5888

Contents lists available at ScienceDirect

Journal of Power Sources

journal homepage: www.elsevier.com/locate/jpowsour

Proton conductive inorganic–organic hybrid membranes functionalized with phosphonic acid for polymer electrolyte fuel cell

Junji Umeda[a], Masashi Suzuki[b], Masaki Kato[b], Makoto Moriya[a], Wataru Sakamoto[a], Toshinobu Yogo[a,*]

[a] Division of Nanomaterials Science, EcoTopia Science Institute, Nagoya University, Furo-cho, Chikusa-ku, Nagoya, Aichi 464-8603, Japan
[b] Research and Development Division, Aichi Industrial Technology Institute, Nishi-shinwari, Hitotsugi-cho, Kariya, Aichi 448-0003, Japan

ARTICLE INFO

Article history:
Received 12 October 2009
Received in revised form 1 December 2009
Accepted 17 December 2009
Available online 29 December 2009

Keywords:
Inorganic–organic hybrid
Proton-conducting membrane
Sol–gel process
Phosphonic acid
Fuel cell

ABSTRACT

Proton conductive sol–gel derived hybrid membranes were synthesized from aromatic derivatives of methoxysilanes and ethyl 2-[3-(dihydroxyphosphoryl)-2-oxapropyl]acrylate (EPA). Two aromatic derivatives of methoxysilanes with different number of methoxy groups were used as the starting materials. Hybrid membranes from difunctional (methyldimethoxysilylmethyl)styrene (MDMSMS(D))/EPA revealed a higher chemical stability and mechanical properties than those from monofunctional (dimethylmethoxysilylmethyl)styrene (DMMSMS(M))/EPA. The membrane–electrode assembly (MEA) using the hybrid membranes as electrolytes worked as a fuel cell at 100 °C under saturated humidity. The DMMSMS(M)/EPA membrane-based MEA showed a larger current density than that from MDMSMS(D)/EPA. On the other hand, the MDMSMS(D)/EPA membrane-based MEA exhibited higher open circuit voltages than the DMMSMS(M)/EPA-based MEA, and was stable during fuel cell operation at 80 °C at least for 48 h.

1. Introduction

Polymer electrolyte fuel cells (PEFCs) are expected to be promising energy sources because of high efficiency and clean exhaust gas. Perfluorosulfonate polymers, such as Nafion and Flemion, are widely used as electrolyte membranes for PEFCs due to their high mechanical strength and proton conductivity. However, the present PEFCs are designed to operate at around 80 °C, as their performance deteriorates at higher temperatures. Operation of PEFCs at temperatures between 100 and 150 °C is favorable for more efficient systems because the cooling system of the fuel cell is simplified and the tolerance of Pt catalyst toward CO increases [1,2]. For these operation conditions, new membranes exhibiting good properties at intermediate temperatures have been required.

The proton transport in the most commonly used perfluorosulfonate polymer membranes is based on a water phase, and this limits the operating temperature. Phosphoric acid has already been used as an electrolyte for phosphoric acid fuel cells (PAFCs) applications around 200 °C, and reveals high proton conductivity based on the structure diffusion [3–5]. However, the incorporation of phosphoric acid to a polymer matrix has a leaching problem, as phosphoric acid molecules are retained in polymer matrices via weak interaction or hydrolytically unstable bonds like C–O–P bond. To avoid the problem, the use of phosphonic acid derivatives has been reported [6,7]. Phosphonic acids are considered to be a promising proton carrier at intermediate temperatures (100–150 °C) because of their good proton donor and acceptor properties. Phosphonic acids are bound via chemically stable C–P bond and contribute to the proton conduction. Furthermore, phosphonic acids have a better thermal stability than sulfonic acid [8,9]. These properties are favorable for fuel cell application at intermediate temperatures.

Inorganic–organic hybrid materials attract attention because of their capacity to produce materials having a wide range of physical, chemical, thermal and mechanical properties due to the beneficial properties of organic and inorganic phase. Proton conductive inorganic–organic hybrids with various acid species have been reported [10–16]. The organosiloxane-based inorganic–organic hybrid membranes consist of siloxane linkages, organic chains and mixed acid species. The inorganic component of siloxane linkages increases the thermal and chemical stabilities of the membrane, and the organic component improves the flexibility. Hence, the hybrid membranes are expected to possess suitable properties for PEFCs at intermediate temperatures. Recently, we have synthesized the proton conductive inorganic–organic hybrid membranes from aromatic derivatives of methoxysilane and ethyl 2-[3-(dihydroxyphosphoryl)-2-oxapropyl]acrylate (EPA) through copolymerization and sol–gel reaction [17]. These membranes consist of organic polymer chain formed by polymerization and siloxane linkage derived from sol–gel reaction of alkoxysilane. The

* Corresponding author. Tel.: +81 52 789 2750; fax: +81 52 789 2121.
E-mail address: yogo@esi.nagoya-u.ac.jp (T. Yogo).

0378-7753/$ – see front matter © 2009 Elsevier B.V. All rights reserved.
doi:10.1016/j.jpowsour.2009.12.078

polymer chain possesses covalently bound phosphonic acid groups, which contribute to proton conduction. The hybrid membranes revealed high thermal stability and stable proton conductivity up to 140 °C. However, the properties of the membrane have not been studied in detail.

This paper describes the characterization of the hybrid membranes synthesized from two kinds of methoxysilane derivatives and EPA. The effects of starting methoxysilane on the membrane structures and properties were investigated. The H_2/O_2 fuel cell performances of membrane–electrodes assemblies (MEAs) were also studied.

2. Experimental procedure

2.1. Membranes

Hybrid membranes were prepared from aromatic derivatives of methoxysilane and ethyl 2-[3-(dihydroxyphosphoryl)-2-oxapropyl]acrylate (EPA) according to our previous study [17]. Two kinds of aromatic derivatives of methoxysilane, (dimethylmethoxysilylmethyl)styrene (DMMSMS) or (methyldimethoxysilylmethyl)styrene (MDMSMS), were used for the preparation of the hybrid membranes. These compounds are abbreviated as DMMSMS (M, monosubstituted) and MDMSMS (D, disubstituted) based on the number of methoxy groups. The samples were labeled with their monomer feed ratio such as DMMSMS(M) (or MDMSMS(D))/EPA = 1/6. The monomer feed ratio of 1/6 was investigated in this study.

2.2. Characterization of membranes

The microstructure of the membrane and MEA was observed with a scanning electron microscope (SEM, JEOL, JSM-5600). Solid-state ^{29}Si and ^{31}P cross-polarization (CP)-magic angle spinning (MAS) nuclear magnetic resonance (CP-MAS NMR) spectra of the hybrid membranes were recorded with an Avance 300 spectrometer (Bruker, Biospin) operating at 59.624 and 121.495 MHz, respectively. The spinning rate of samples was set to 5.0 kHz. The external standards for ^{29}Si and ^{31}P chemical shift were hexamethylcyclotrisiloxane and ammonium phosphate monobasic. A differential scanning calorimeter (DSC, Shimadzu, DSC-60) was used to measure the melting curves of water in the hybrid membranes. The samples were kept at 40 °C under 100% relative humidity for more than 1 h before measurements. The DSC curves were obtained for the samples from −80 to 60 °C at a heating rate of 3 °C min^{-1}. The chemical stability of the membranes was examined through immersing small pieces of membrane in Fenton's reagent (3% H_2O_2 aqueous solution with 2 ppm $FeSO_4$) at 80 °C [18].

The mechanical properties of the hybrid membranes were evaluated using a Knoop microindentation tester with a microindenter (Akashi, MVK-E). The applied load and time were 245 mN and 20 s, respectively. All the samples were kept under ambient conditions before measurements. The elastic modulus (E) was calculated from the values of the Knoop hardness (μHK), as reported [19].

2.3. Preparation of electrodes and membrane–electrodes assemblies (MEAs)

The catalyst ink was prepared by mixing 5% Nafion® solution (Wako Chemical), Pt/C powder (N.E. Chemcat) and methanol. The mixing suspension was stirred with ultrasonication for 30 min to obtain a catalyst ink, and then uniformly casted on carbon paper coated with Ketchen black. The amounts of Pt and Nafion ionomer in the electrode were 0.5 mg cm^{-2} and 0.8 mg cm^{-2}, respectively. MEAs were prepared by hot press at 120 °C for 4 min to combine the electrodes and membrane.

2.4. Single cell test

The MEA was incorporated into a single cell test fixture. The current–voltage curves were measured by using a potentiometer (Solartron, SI 1287) under 0.1 L min^{-1} H_2 and O_2 flow for anode and cathode, respectively. The cell temperature was set to be at 80 and 100 °C and humidification of feed H_2/O_2 gases was conducted by bubbling the gases through distilled water at 80 and 100 °C. The cell performance under low relative humidity (RH) was also evaluated at 120 °C by feeding humidified H_2 (100 °C) and O_2 (100 °C). The RH at the conditions was calculated to be 51% RH.

Durability test of the cell was carried out at a constant current density of 40 mA cm^{-2} at 80 °C. The test was interrupted every 8 h. To interrupt the test, the reactant flows were stopped and the system was cooled to room temperature. The test was restarted after the system reached the required temperature.

The cell impedance was also measured by ac impedance method using a Solartron SI 1255 frequency response analyzer equipped with the SI 1287 electrochemical interface from 1 MHz to 10 mHz. The proton conductivity (σ) was determined using the relation $\sigma = l/RS$, where l is the thickness of the membrane, R is the measured resistance of the membrane and S is the surface area of the electrode.

3. Results and discussion

3.1. Appearance and microstructure of the hybrid membranes

Two kinds of hybrid membranes were prepared with a monomer feed ratio of DMMSMS(M)/EPA = 1/6 or MDMSMS(D)/EPA = 1/6, since the membranes showed the highest conductivities at the Si/P = 1/6 ratio. These membranes were self-standing, transparent and yellowish. Fig. 1(a) and (b) show the appearances of DMMSMS(M)/EPA = 1/6 and MDMSMS(D)/EPA = 1/6 hybrid membranes, respectively. Self-standing membranes with a thickness of less than 100 μm can be readily obtained. Fig. 1(c) and (d) shows SEM images of the hybrid membranes with the compositions of DMMSMS(M)/EPA = 1/6 and MDMSMS(D)/EPA = 1/6, respectively. Generally, a sample synthesized by sol–gel method forms a crack and fracture due to shrinkage during drying process. However, the surfaces of the hybrid membranes are smooth, and have no apparent crack and void. The result indicates that the organic moieties in hybrid membranes adjust the drying rate to suppress the local and rapid shrinkage, leading to the homogeneous membranes at the micrometer level.

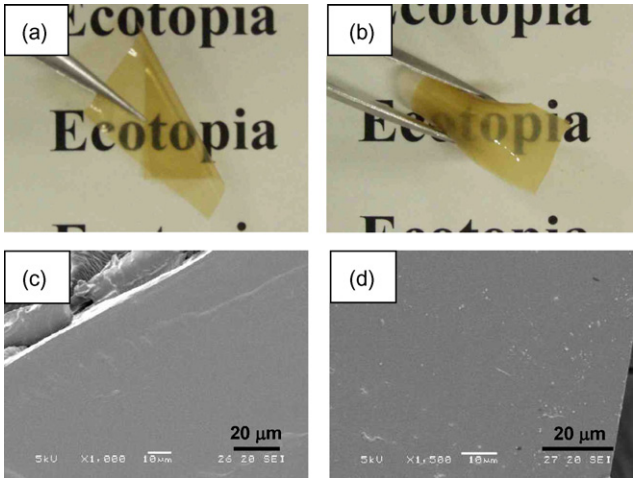

Fig. 1. Appearance and microstructure of hybrid membranes: (a) DMMSMS(M)/EPA = 1/6, (b) MDMSMS(D)/EPA = 1/6, (c) DMMSMS(M)/EPA, and (d) MDMSMS(D)/EPA hybrid membrane.

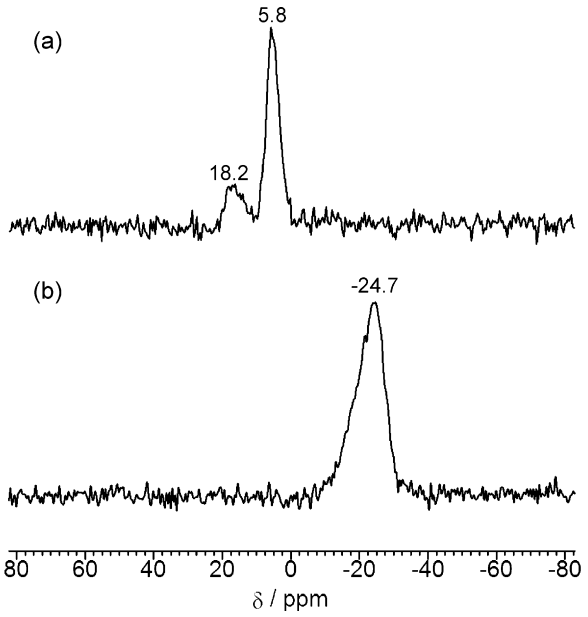

Fig. 2. ^{29}Si NMR spectra of hybrid membranes: (a) DMMSMS(M)/EPA = 1/6 hybrid membrane and (b) MDMSMS(D)/EPA = 1/6 hybrid membrane.

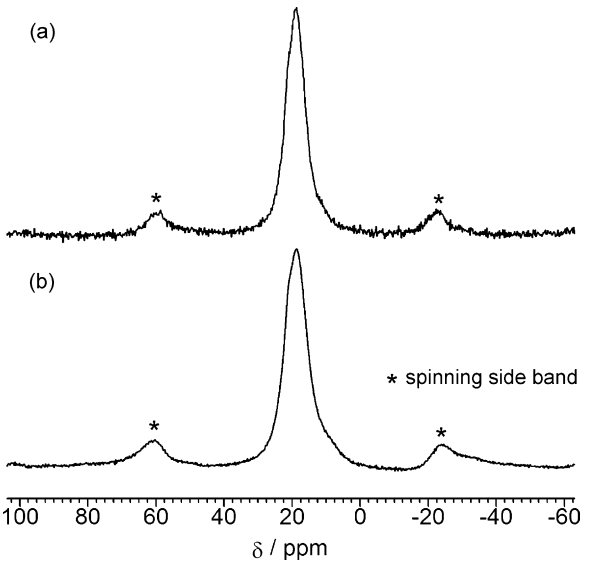

Fig. 3. ^{31}P NMR spectra of hybrid membranes: (a) DMMSMS(M)/EPA = 1/6 hybrid membrane and (b) MDMSMS(D)/EPA = 1/6 hybrid membrane.

3.2. NMR analysis of the hybrid membranes

Fig. 2 shows ^{29}Si NMR spectra of the DMMSMS(M)/EPA and MDMSMS(D)/EPA hybrid membranes with a Si/P monomer feed ratio of 1/6. The silicate structures derived from DMMSMS(M) and MDMSMS(D) are represented by M^n and D^n notation, respectively. The superscript indicates the total number of siloxane bonds attached to the R_3SiO or R_2SiO_2 tetrahedron. The spectrum of the DMMSMS(M)/EPA membrane consists of two signals at 18.2 and 5.8 ppm (Fig. 2(a)). A small signal at 18.2 ppm is assigned to M^0 unit, while a large signal at 5.8 ppm is M^1 unit [20]. For MDMSMS(D)/EPA hybrid membrane, a broad signal is observed at −24.7 ppm as shown in Fig. 2(b). The broad signal is composed mainly of D^2 signal together with D^1 at the lower field side. From these results, the Si–OCH_3 bond in the starting compounds undergoes hydrolysis and condensation yielding Si–O–Si linkages in the hybrid membranes. DMMSMS(M) has one methoxy group, which form dimeric Si–O–Si linkage through hydrolysis and condensation reactions. On the other hand, two methoxy groups of MDMSMS(D) form linear Si–O–Si linkage. In MDMSMS(D)/EPA membrane, the density of Si–O–Si linkage is higher than that of DMMSMS(M)/EPA membrane. In the present synthesis, the sol–gel condensation was conducted to form silica structures, after the organic polymer chain was synthesized. The high molar ratio of P to Si (6/1) corresponds to the high ratio of organic polymer chain. Even at the high ratio of organic polymer phase, the silica linkage was formed successfully in the organic polymer matrix by sol–gel condensation reaction.

Fig. 3 shows the ^{31}P CP-MAS NMR spectra of hybrid membranes from DMMSMS(M)/EPA = 1/6 and MDMSMS(D)/EPA = 1/6. The profile of each spectrum is almost the same to each other. In both spectra, single ^{31}P resonance signals were observed at 18.7 ppm. The signals are attributed to the phosphonic acid group (–PO_3H_2) bound with polymer backbone, since free H_3PO_4 appears at 0 ppm. The only one signal in the spectra indicates that all phosphonic acid groups in the membranes did not form other bonds such as Si–O–P. Silicon alkoxide does not react with P–OH during sol–gel process at low temperatures [21]. Therefore, these phosphonic acid groups in the hybrid membranes can contribute to proton conduction.

Fig. 4 depicts the possible structures of DMMSMS(M)/EPA and MDMSMS(D)/EPA hybrid membranes. The number of methoxy groups in the starting organoalkoxysilanes affects the structure of the hybrid membrane as described above. Methoxy groups of DMMSMS(M) or MDMSMS(D) undergo hydrolysis to form Si–O–Si linkages. DMMSMS(M) includes one methoxy group to yield dimeric Si–O–Si cross-linking after sol–gel reaction. In contrast, as MDMSMS(D) has two methoxy groups, linear Si–O–Si linkages are formed in MDMSMS(D)/EPA membrane. Both hybrid membranes contain covalently bound phosphonic acid groups in polymer chain formed by copolymerization reaction between aromatic derivatives of methoxysilane and EPA. Immobilization of phosphonic acid via hydrolytically stable C–P bond is desirable for the suppression of leach-out of phosphonic acid groups.

3.3. The chemical stability of the membranes

The oxidation stability of the membranes was examined using Fenton's reagent at 80 °C. The DMMSMS(M)/EPA = 1/6 membrane broke into pieces by shaking after 5 h, and then almost dissolved in 7 h. On the other hand, the membranes of MDMSMS(D)/EPA = 1/6 maintained the dimension with no visible crack even after 24 h treatment. Also, the membrane did not show any distinct change in the FT-IR spectrum. The results indicate that the MDMSMS(D)/EPA membrane has a much higher stability to oxidation than the DMMSMS(M)/EPA membrane due to the two-dimensional siloxane linkage. However, the DMMSMS(M)/EPA membrane also have relatively high anti-oxidative stability, which was comparable to that of aromatic polymer electrolytes [18,22]. Therefore, the anti-oxidative properties of the membranes can be improved by the incorporation of Si–O network.

3.4. DSC analysis of the hybrid membranes

A differential scanning calorimetry (DSC) was used to investigate the state of water in the hybrid membranes. DSC has been used extensively to characterize the phase transition of water in the water-containing systems [23–25]. Fig. 5 shows DSC heating curves for the hybrid membranes. The endothermic peaks observed above 0 °C correspond to the melting of absorbed water on the surface of the membrane powders. The distinct endothermic peaks are observed for both samples below 0 °C. For the DSC curve of DMMSMS(M)/EPA hybrid membrane, an endothermic peak starts at −26.2 °C and has the maximum at −8.2 °C. While the curve of

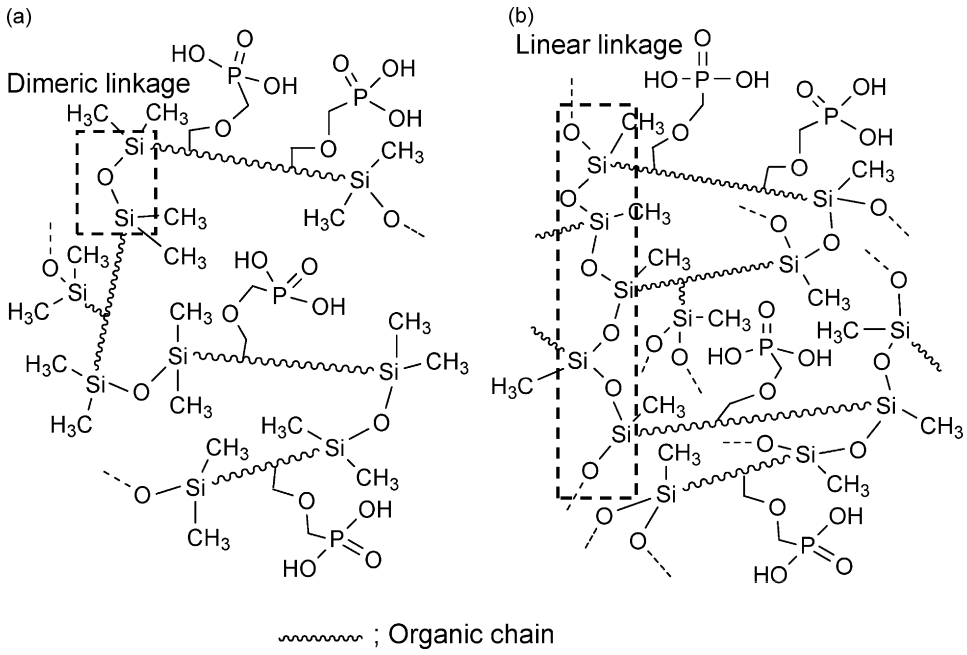

Fig. 4. Possible structures of hybrid membranes: (a) membrane from monofunctional DMMSMS(M)/EPA = 1/6 and (b) membrane from difunctional MDMSMS(D)/EPA = 1/6.

MDMSMS(D)/EPA hybrid membrane shows an endothermic peak at the lower temperature; the onset and top of the peak are −28.6 and −9.1 °C, respectively. The endothermic peaks are attributed to the melting of water in the hybrid membranes. The melting and freezing temperatures of water confined in small pores are lower than those of free water. The DSC results indicate that the absorbed water in the hybrid membranes is confined in small pores, as the peak temperatures are much lower than the melting point of free water. Moreover, the results also indicate that the size of water domain for MDMSMS(D)/EPA hybrid membrane is smaller than that for DMMSMS(M)/EPA hybrid membrane. The MDMSMS(D)/EPA hybrid membrane has dense Si–O–Si linkages compared to the DMMSMS(M)/EPA membrane as shown in Section 3.2. Therefore, the difference in structure may affect the water domain size of the hybrid membranes. The water domain in proton exchange membranes plays an important role in the proton transport. The smaller water domain in MDMSMS(D)/EPA hybrid membrane may suppress the proton conduction, leading to the low proton conductivity as reported; the conductivities at 40 °C under 100% RH are 1.6×10^{-2} and 4.1×10^{-3} S cm^{-1} for DMMSMS(M)/EPA = 1/6 and MDMSMS(D)/EPA = 1/6 hybrid membrane, respectively [17].

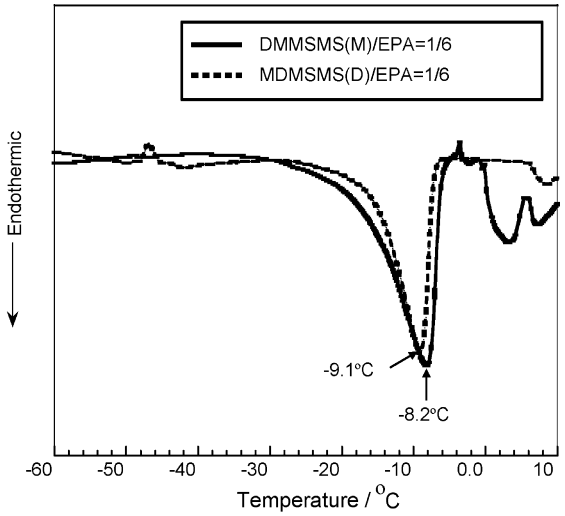

Fig. 5. DSC heating curves for DMMSMS(M)/EPA = 1/6 and MDMSMS(D)/EPA = 1/6 hybrid membranes. The samples were pre-treated at 40 °C under 100% relative humidity.

3.5. Mechanical strength of the hybrid membranes

The Knoop indentation tests were performed to investigate the mechanical properties of the hybrid membranes. The results are summarized in Table 1. The measurements were conducted on the samples kept under ambient conditions for more than a month. The Knoop microhardness (μHK) and the elastic modulus of the MDMSMS(D)/EPA = 1/6 hybrid membrane are larger than those of the DMMSMS(M)/EPA = 1/6 hybrid membrane. The increase in the μHK and *E* are attributed to an increase of Si–O–Si density in the hybrid membrane. The two-dimensional Si–O–Si linkage in the MDMSMS(D)/EPA membrane is the reason for the higher μHK and *E* than that those of DMMSMS(M)/EPA membrane as described in Section 3.2. The μHK and *E* values of the MDMSMS(D)/EPA = 1/6 hybrid membrane are comparable to those of polycarbonate (μHK (micro-Vickers hardness): 0.14 GPa; *E*: 2.3 GPa) [19]. DMMSMS(M)/EPA = 1/6 hybrid membrane having the lower μHK and *E* values is more flexible as shown in Fig. 1. Although there are differences in the mechanical properties between the DMMSMS(M)/EPA and MDMSMS(D)/EPA hybrid membrane, both membranes possess the sufficient mechanical strength for the fabrication of test cell in Section 3.6.

3.6. Cell performances of the MEAs

Fig. 6 shows potential–current polarization curves of the single cells using the DMMSMS(M)/EPA = 1/6 and MDMSMS(D)/EPA = 1/6

Table 1
Knoop microhardness (μHK) and elastic modulus (*E*) of the hybrid membranes.

Membrane	μHK (GPa)	*E* (GPa)
DMMSMS(M)/EPA = 1/6	0.054	0.78
MDMSMS(D)/EPA = 1/6	0.082	2.7

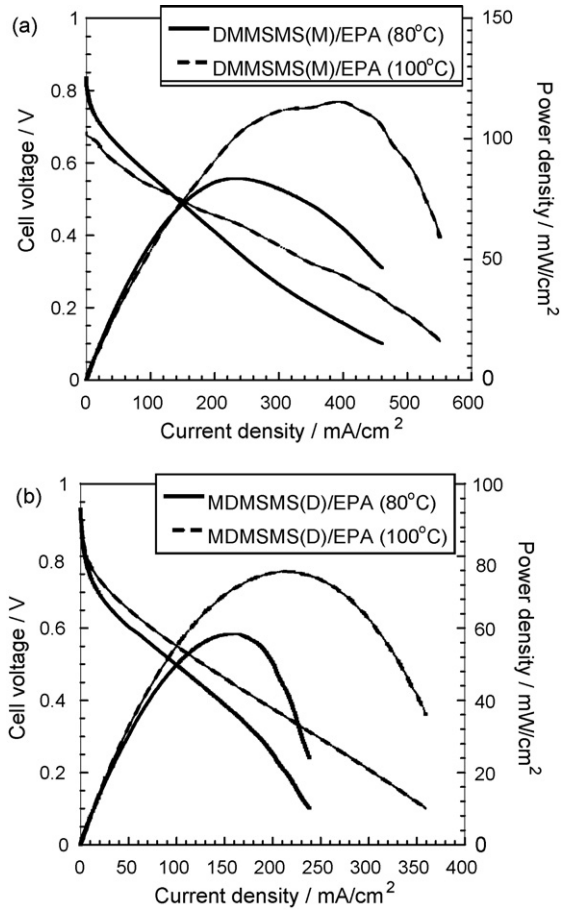

Fig. 6. Cell performances of MEAs from hybrid membranes at 80 and 100 °C under saturated humidity. (a) Cell performances for DMMSMS(M)/EPA = 1/6 membrane-based MEA and (b) cell performances for MDMSMS(D)/EPA = 1/6 membrane-based MEA.

membrane at 80 and 100 °C under saturated humidity. The membrane thicknesses of the former and the latter were 40 and 50 μm, respectively. Both cells worked as a fuel cell at 80 and 100 °C, and a larger current density was observed for the cell using the DMMSMS(M)/EPA membrane as an electrolyte. The maximum power densities of the cells using the DMMSMS(M)/EPA and MDMSMS(D)/EPA were 115 and 76 mW cm^{-2}, respectively, at 100 °C. However, when the temperature increased from 80 to 100 °C, the open circuit voltage (OCV) of the cell based on the DMMSMS(M)/EPA dropped from 0.84 V to 0.69 V (Fig. 6a). Both the initial low OCV and the decrease in OCV might be attributed to gas cross-over or internal micro-short circuit due to a loss in mechanical strength of the membrane at the high temperature under fully humidified condition. By contrast, the OCVs over 0.9 V were observed for the cell using the MDMSMS(D)/EPA under both conditions at 80 and 100 °C. It indicates that the MDMSMS(D)/EPA membrane possesses a higher thermal and mechanical stability than DMMSMS(M)/EPA under these conditions due to the dense silica structure as described above.

Fig. 7shows the impedance spectra of the cells operated at 80 °C under saturated humidity. The impedance spectra show almost a semicircle. The intersection at the real axis and the diameter of the semicircle correspond to the internal resistance and charge transfer resistance, respectively. The internal resistances of the cells for the DMMSMS(M)/EPA membrane at 100 and 80 °C were 0.084 and 0.192 Ω cm^2, respectively. The internal resistances for MDMSMS(D)/EPA-based cells at 100 and 80 °C were 1.03 and 1.78 Ω cm^2, respectively, which were higher than

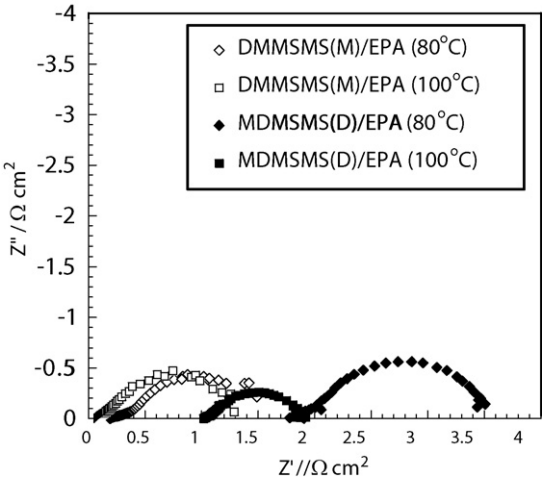

Fig. 7. Impedance spectra of MEAs from hybrid membranes at 80 and 100 °C under saturated humidity. Measurements were taken at 0.4 V. (□ and ◊) DMMSMS(M)/EPA = 1/6 and (■ and ♦) MDMSMS(D)/EPA = 1/6.

those for DMMSMS(M)/EPA. The cell resistance includes ionic resistance and electrode resistance. When the electrode resistance is assumed to be negligibly small, the proton conductivities of DMMSMS(M)/EPA in the MEA are calculated to be 4.8×10^{-2} and 2.1×10^{-2} S cm^{-1} at 100 and 80 °C, respectively. Similarly, the proton conductivities of MDMSMS(D)/EPA in the MEA are 4.9×10^{-3} and 2.8×10^{-3} S cm^{-1} at 100 and 80 °C, respectively. The calculated conductivities at 80 °C from the MEA experiment are smaller than those previously reported (4.2×10^{-2} and 1.5×10^{-2} S cm^{-1} for the DMMSMS(M)/EPA and MDMSMS(D)/EPA membrane, respectively, at 80 °C [17]). This difference may be due to the use of different measurement methods. In the previous work, the conductivities of membranes were measured with platinum electrodes under static atmosphere in a chamber. Since Nafion solution was used to form three phase interface in the current MEAs, the hybrid membranes were sandwiched between Nafion-coated Pt/C electrodes. The compatibility between the Nafion ionomer and the hybrid membranes is not necessarily good due to their different chemical natures. The resistances obtained in this study include the membrane resistance and contact resistance, which might result in the larger cell internal resistance. Nafion used as a binder in the electrodes is not compatible with many other polymers, which leads to the higher resistance at the interface [26]. A cell performance depends strongly on the MEA fabrication parameters, such as kinds and amounts of electrolyte binders, kinds of gas diffusion layers, conditions of hot press, and so on [27–29]. The fabrication method of the MEAs must be optimized to improve the cell performance. One way to obtain a MEA exhibiting higher performance is to replace the Nafion solution used for the electrode impregnation with the polymer solution of the same chemical composition as that of the membrane [30].

The cell performance at a higher temperature under low humidity was evaluated for the MDMSMS(D)/EPA membrane-based MEA, because the MEA revealed a better stability than that from the DMMSMS(M)/EPA membrane. Fig. 8 shows a polarization curve of the cell using the MDMSMS(D)/EPA membrane measured at 120 °C at 51% RH. The result confirms that the cells using the hybrid membrane worked as a fuel cell at 120 °C under the low relative humidity. However, the performance abruptly dropped compared to the performance at 100 °C under fully humidified condition. The decline in performance is ascribed to decrease in conductivity of the membrane under low relative humidity and the use of Nafion ionomer in catalyst layer of the MEA. We have reported the conductivities of the hybrid membranes under low relative humidities

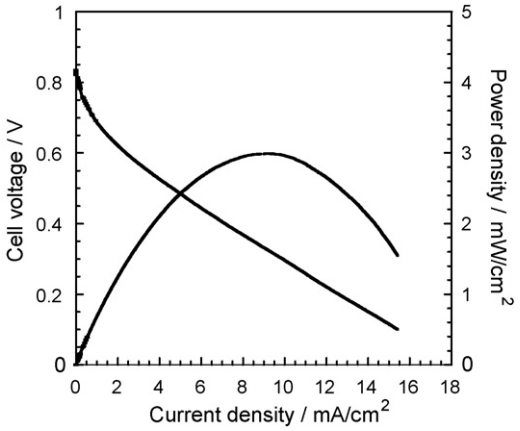

Fig. 8. Cell performance of MEA using the DMMSMS(D)/EPA membrane at 120 °C and 51% RH.

[17], which were comparable with those reported [14,15]. The relatively low conductivities of the hybrid membranes under low humidified conditions must be improved for an actual operation at intermediate temperatures. This will require the increase in volume fraction of phosphonic acid as high as possible to provide a good connectivity within the hydrated hydrophilic domains at low humidified conditions [6]. It seems to be achievable for hybrid membranes having a dense structure (e.g. MDMSMS(D)/EPA membranes) to introduce higher contents of phosphonic acid group. On the other hand, the use of Nafion ionomer in catalyst layer of the MEA is also the reason for the low performance because the properties of Nafion deteriorate at high temperatures. New ionomers possessing a better compatibility with the membranes and prominent properties at high temperatures are required for the improvement of the cell performance.

The durability test was conducted on the cell using MDMSMS(D)/EPA membrane at 80 °C under saturated humidity. Fig. 9 shows the cell voltage as a function of time operated at a constant current density of 40 mA cm^{-2}. The measurement was interrupted every 8 h and total time of the test was 48 h. The cell kept the performance of cell voltage of 0.6–0.7 V, indicating a good stability of the hybrid membrane for 48 h. The time and current density for the current membrane are superior to those reported for SiO_2-based inorganic–organic hybrid membrane [27]. Although significant drops in cell voltage were not observed over the time

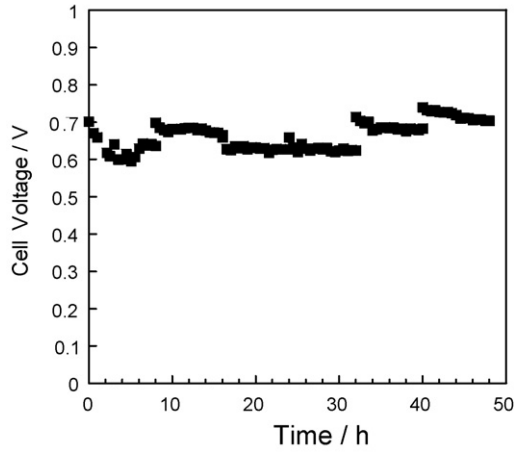

Fig. 9. Change in cell voltage for MDMSMS(D)/EPA = 1/6 membrane-based MEA with time operated at constant current density of 40 mA cm^{-2} at 80 °C under saturated humidity. The test was interrupted every 8 h.

range of 48 h, the variations in cell voltage were observed at restarting points every 8 h. The polarization curve of the cell after the durability test for 48 h exhibited a higher performance than that before the test (not shown). The power densities of the cell before and after the test were 50 and 56 mW cm^{-2} at 0.5 V, respectively. The improvement probably derived from the improved structure of the interface between the membrane and catalyst layer through the repeated start-up/shut-down (heating/cooling) operations. These results also indicate that the fabrication method of the MEA must be optimized to achieve the further improvement of performance.

4. Conclusions

Inorganic–organic hybrid membranes synthesized from DMMSMS(M)/EPA and MDMSMS(D)/EPA, and their properties were investigated. The siloxane linkage (Si–O–Si) formed in hybrid membranes depended on the number of methoxy group in starting alkoxysilanes. The higher chemical stability and mechanical properties of MDMSMS(D)/EPA membrane reflected the two-dimensional Si–O–Si linkage, which depended on the number of methoxy groups in the starting methoxysilanes. The high conductivity of DMMSMS(M)/EPA membrane was attributed to the larger size of water in the membrane. The maximum power density of the cells using DMMSMS(M)/EPA and MDMSMS(D)/EPA were 115 and 76 mW cm^{-2}, respectively, at 100 °C and saturated humidities. In contrast, MDMSMS(D)/EPA hybrid membrane-based MEA kept the high performance even at 100 °C under fully humidified condition due to its high mechanical property. The MEA also exhibited a good stability during fuel cell operation at 80 °C at least for 48 h.

References

[1] Q.F. Li, R.H. He, J.O. Jensen, N.J. Bjerrum, Chem. Mater. 15 (2003) 4896–4915.
[2] C. Wieser, Fuel Cells 4 (2004) 245–250.
[3] K. Kordesch, G. Simader, Fuel Cells and Their Applications, VCH, Weinheim, 1996.
[4] M.E. Schuster, W.H. Meyer, Annu. Rev. Mater. Res. 33 (2003) 233–261.
[5] T. Dippel, K.D. Kreuer, J.C. Lassegues, D. Rodriguez, Solid State Ionics 61 (1993) 41–46.
[6] H. Steininger, M. Schuster, K.D. Kreuer, A. Kaltbeitzel, B. Bingol, W.H. Meyer, S. Schauff, G. Brunklaus, J. Maier, H.W. Spiess, Phys. Chem. Chem. Phys. 9 (2007) 1764–1773.
[7] M. Schuster, K.D. Kreuer, H. Steininger, J. Maier, Solid State Ionics 179 (2008) 523–528.
[8] E. Parcero, R. Herrera, S.P. Nunes, J. Membr. Sci. 285 (2006) 206–213.
[9] M. Schuster, T. Rager, A. Noda, K.D. Kreuer, J. Maier, Fuel Cells 5 (2005) 355–365.
[10] D.R. Vernon, F.Q. Meng, S.F. Dec, D.L. Williamson, J.A. Turner, A.M. Herring, J. Power Sources 139 (2005) 141–151.
[11] J.D. Kim, I. Honma, Electrochim. Acta 49 (2004) 3429–3433.
[12] Y. Park, M. Nagai, Solid State Ionics 145 (2001) 149–160.
[13] T. Tezuka, K. Tadanaga, A. Hayashi, M. Tatsumisago, J. Electrochem. Soc. 156 (2009) B174–B177.
[14] Y. Daiko, K. Ogura, K. Katagiri, H. Muto, M. Sakai, A. Matsuda, Solid State Ionics 179 (2008) 1166–1169.
[15] M. Aparicio, J. Mosa, A. Duran, J. Sol–Gel Sci. Tehnol. 40 (2006) 309–315.
[16] J.C. Lassegues, J. Grondin, M. Hernandez, B. Maree, Solid State Ionics 145 (2001) 37–45.
[17] J. Umeda, M. Moriya, W. Sakamoto, T. Yogo, Electrochim. Acta 55 (2009) 298–304.
[18] K. Miyatake, N. Asano, M. Watanabe, J. Polym. Sci. Pol. Chem. 41 (2003) 3901–3907.
[19] P. Innocenzi, M. Esposto, A. Maddalena, J. Sol–Gel Sci. Technol. 20 (2001) 293–301.
[20] S.E. Rankin, C.W. Macosko, A.V. McCormick, J. Polym. Sci. Pol. Chem. 35 (1997) 1293–1302.
[21] S.P. Szu, L.C. Klein, M. Greenblatt, J. Non-Cryst. Solids 143 (1992) 21–30.
[22] B.J. Liu, D.S. Kim, J. Murphy, G.P. Robertson, M.D. Guiver, S. Mikhailenko, S. Kaliaguine, Y.M. Sun, Y.L. Liu, J.Y. Lai, J. Membr. Sci. 280 (2006) 54–64.
[23] K. Ishikiriyama, M. Todoki, T. Kobayashi, H. Tanzawa, J. Colloid Interface Sci. 173 (1995) 419–428.

[24] K. Ishikiriyama, M. Todoki, K. Motomura, J. Colloid Interface Sci. 171 (1995) 92–102.
[25] M. Iijima, Y. Sasaki, T. Osada, K. Miyamoto, M. Nagai, Int. J. Thermophys. 27 (2006) 1792–1802.
[26] R. Thangamuthu, C.W. Lin, J. Power Sources 150 (2005) 48–56.
[27] R. Thangamuthu, C.W. Lin, J. Power Sources 161 (2006) 160–167.
[28] Y. Komoda, K. Okabayashi, H. Nishimura, M. Hiromitsu, T. Oboshi, H. Usui, J. Power Sources 193 (2009) 488–494.
[29] T. Frey, M. Linardi, Electrochim. Acta 50 (2004) 99–105.
[30] S. Besse, P. Capron, O. Diat, G. Gebel, F. Jousse, D. Marsacq, M. Pineri, C. Marestin, R. Mercier, J. New Mater. Electrochem. Syst. 5 (2002) 109–112.